

Traffic Signal Optimization Based on Fuzzy Control and Differential Evolution Algorithm

Haifeng Lin^{ID}, Yehong Han^{ID}, Weiwei Cai^{ID}, *Member, IEEE*, and Bo Jin^{ID}

Abstract—Urban traffic congestion is often concentrated at urban intersections. An urban road traffic signal control system is needed to prevent problems such as driving delays caused by frequent traffic congestions on trunk lines, exhaust emissions owing to frequent start and stop of vehicles, and fuel wastage due to long idling times. Maximizing the traffic capacity of an intersection and reducing the delay rate of vehicles has always been a problem for traffic control research. The coordinated control of urban traffic signals is regarded as a multi-objective optimization problem. A mathematical model for urban trunk traffic is studied herein. An average delay model, average queue length model, total delay calculation model for vehicles at intersections, and vehicle exhaust emission model are established to obtain an optimization model for a new traffic trunk coordinated control system. In addition, our study combines the fuzzy control theory with the adaptive sequencing mutation multi-objective differential evolution algorithm (FASM-MDEA). This new optimization method for traffic signal control at urban intersections is proposed as a solution for the traffic flow optimization model to solve the problem of traffic signal coordination and control of urban trunk lines. The simulation results demonstrate the effectiveness of the model optimization algorithm proposed in this study.

Index Terms—Urban traffic signal, coordinated control, multi-objective optimization, fuzzy control, adaptive sorting mutation, differential evolution algorithm (DEA).

I. INTRODUCTION

THE main reason for urban traffic congestion is the traffic demand that exceeds the current urban traffic service

Manuscript received 10 December 2021; revised 11 May 2022 and 24 June 2022; accepted 27 July 2022. Date of publication 16 August 2022; date of current version 2 August 2023. This work was supported in part by the Key Research and Development Plan of Jiangsu Province under Grant BE2021716, in part by the Jiangsu Modern Agricultural Machinery Equipment and Technology Demonstration and Promotion Project under Grant NJ2021-19, in part by the Key Research and Development Program of Shandong Province under Grant 2019GSF108010, and in part by the Postgraduate Scientific Research Innovation Project of Hunan Province under Grant QL20210212. The Associate Editor for this article was W. Wei. (*Corresponding author: Yehong Han.*)

Haifeng Lin is with the College of Information Science and Technology, Nanjing Forestry University, Nanjing 210037, China (e-mail: haifeng.lin@njfu.edu.cn).

Yehong Han is with the College of Information Science and Engineering, Qilu Normal University, Jinan 250200, China (e-mail: 20152176@qlnu.edu.cn).

Weiwei Cai is with the School of Logistics and Transportation, Central South University of Forestry and Technology, Changsha 410004, China, and also with the AiTech Artificial Intelligence Research Institute, Changsha 410000, China (e-mail: vivitsai@ieee.org).

Bo Jin is with the Department of Electrical and Computer Engineering and the Institute of Systems and Robotics, University of Coimbra, 3030-290 Coimbra, Portugal (e-mail: jin.bo@isr.uc.pt).

Digital Object Identifier 10.1109/TITS.2022.3195221

capacity in specific periods of time. The total travel time is one of the most important issues affecting travelers. Because the urban road network consists of road sections and intersections connecting different roads, the total travel time for urban motor vehicles consists of two parts: road section travel time and intersection waiting time (or delay). The travel time on road sections is mainly determined by the road's condition, driving speed of the vehicle, and driving speed of other vehicles on the same road. The delay time at intersections is mainly determined by the traffic geometric conditions of the intersection itself, the traffic demand in all directions, and the traffic control mode at the intersection [1]. In an urban road network, the randomness of traffic demand is one of the main reasons for the uncertainty in vehicle travel time. Specifically, at intersections, the uncertainty of traffic demand, vehicle driving path, and lane selection directly lead to the randomness of the vehicle queuing process. Therefore, the uncertainty of vehicle travel time largely depends on the delay time of vehicles at intersections, which is mainly determined by the traffic demand, road use mode, and traffic control mode at these intersections. Unreasonable traffic control at intersections further aggravates the problem of traffic congestion [2], [3]. As these are critical nodes for traffic assembly and evacuation, improving the traffic service capacity at these intersections is the key to solving urban traffic congestion [4].

Traffic congestion should be addressed considering the intersections. New strategies for intersection control mode are needed to control a large number of intersections, minimize delay, and improve traffic capacity and safety, as intersections are of great practical significance when solving current traffic problems. To alleviate traffic congestion at intersections, it is necessary to comprehensively and accurately estimate their service capacity under various traffic conditions [5]. The traffic congestion at these intersections is directly reflected in the long queues and waiting time, which leads to more waste of time and fuel. In practical applications, queue length and delay index are used as effective tools to monitor the operation of a single traffic movement from a single intersection to the entire traffic network [6]. The estimation of vehicle queue length and delay is helpful to effectively evaluate the target control strategy to identify the problems in traffic control to help decision makers further improve traffic control methods and strategies. For road users, the delay estimation of vehicles at intersections can also help them make the best travel decision and choose the best travel time and paths to avoid unnecessary delays and high travel costs. Therefore, the queue length and

delay of vehicles at the intersection are important indicators for evaluating the operation efficiency and service level. These not only directly evaluate the traffic service level at intersections, the rationality of lane design, fuel consumption, and emissions but also reflects the degree of obstruction of road users and their perception of the service quality at the intersection [7], [8]. Because the traffic system is a nonlinear, time-varying, and lagging large-scale system, it is difficult to obtain satisfactory results using traditional control methods. Therefore, in this study, we make use of the fuzzy control theory and intelligent optimization methods, take a single intersection and trunk road signal control as the research object, and perform a series of in-depth and detailed discussions on the control mode and optimization algorithm; some phased research results are obtained.

The specific contributions of this study are as follows:

(1) A multi-objective traffic organization optimization model of a signalized intersection with the objectives of maximizing capacity, minimizing both average delay, and vehicle density in the target area is established and solved.

(2) Based on the fuzzy control theory and multi-objective differential evolution algorithm (DEA), a traffic signal control algorithm for urban intersections based on traffic intensity is proposed.

(3) To overcome the unreasonable shortcomings of manually determining the membership function of fuzzy controller variables and fuzzy control rules, a method using a DEA to optimize the membership function and fuzzy control rules is proposed.

(4) A traffic signal coordination control method for adjacent intersections is proposed. The traffic flow conditions of each phase of the intersection are integrated to determine the candidate green light phase, and whether to extend the current green light phase is determined by fuzzy reasoning.

The remainder of this paper is organized as follows. Section 2 discusses related work and is followed by a discussion of the design of the HFC of regional intersections in Section 3. A traffic signal multi-objective optimization control model is proposed in Section 4. Section 5 discusses the realization of fuzzy adaptive sequencing mutation multi-objective differential evolution algorithm (FASM-MDEA) for signal control, coordination, and optimization of urban intersections. Section 6 presents the simulation experimental results and analysis, and Section 7 concludes the paper with a summary and future research directions.

II. RELATED WORK

An intersection is the basic unit of an urban road network. Research on intersection signal control is the foundation of urban traffic system research. In general, according to the signal control range, intersection control can be divided into point, line, and area control. Point control is the independent control of an urban road-level intersection without considering the coordination relationship with adjacent intersections. Its purpose is to reduce the traffic delay at the intersection as much as possible. This is the basis of a traffic control system [9]. Wire control is used to control the signal of urban traffic trunk lines with multiple plane intersections.

The control schemes of each intersection are coordinated with each other so that the motorcade entering the trunk line can pass through the trunk line without or as few red lights as possible when driving at a certain speed. Area control is used to control the signal of a plane intersection in a certain area of the city. Starting from the strategic goal of the entire system and according to the traffic volume detection data, it coordinates the traffic signal timing of each intersection in the area, with the goal of achieving the overall optimal effect [10]. If the intersection has adopted the real-time intelligent control method, and then the wire control system is designed according to the traditional method of adjusting the phase difference, it will inevitably lead to an increase in control parameters and the complexity of control methods. When we analyzed and researched some classical traffic control optimization systems, we found that in urban traffic control, fixed-period control is simple and effective when the traffic flow is small and stable. When traffic is crowded and changes significantly, dynamic feedback control should be adopted to reduce vehicle delays. This control mode requires the use of a mathematical model to describe the traffic signal control system [11]. However, the nonlinearity and randomness of traffic systems make modeling very difficult. Therefore, the optimal goal pursued in dynamic feedback control is often difficult to achieve. Artificial intelligence, such as intelligent algorithms, fuzzy theory, and machine learning, have attracted increasing attention. At present, fuzzy logic is a mature method for responding to vehicle traffic signal control, and has been successfully applied to the theoretical research of traffic signal control systems. The advantage of fuzzy control is that it does not need to obtain a complex relationship in the model to establish an accurate mathematical model. It is a rule-based intelligent control method that is especially suitable for urban traffic control systems with great randomness [12], [13]. The DEA realizes global and fast search in solution space by using the principle of natural evolution. It is widely used to solve large-scale combinatorial optimization problems. When solving the problem of model design and calculation in real-time traffic control systems, a DEA can be used to carry out a global search and determine the common cycle, or to solve the optimal cooperation problem of intersection signal control schemes in regional control systems, so as to effectively avoid the possible combination contradiction of traffic schemes.

In recent years, many researchers have found that the integration of traffic signal control and dynamic traffic guidance can more effectively alleviate urban traffic congestion. The integration of the two has become one of the hotspots of urban traffic system research and the development trend of urban traffic control [14]. Jafari *et al.* [15] propose a novel stable predictive controller for urban traffic, and state-space dynamics are used to estimate the number of vehicles at an isolated intersection and the length of its queue. This is a novel control strategy based on the type of traffic light and on the duration of the green-light phase and aims to achieve an optimal balance at intersections. Liu *et al.* [16] establish to solve the intersection vehicle delay and parking times, and to establish an intersection signal control model with the minimum parking times and delay as the optimization

objective. Taking the phase saturation as the index of the control effect and considering the influence of speed guidance on the vehicle running state, they establish an optimization model of road intersection signal control in a vehicle road coordination environment. Li *et al.* [17] study the adaptive optimal control method of a single-point signalized intersection, establish the logical architecture of an information interaction network for urban single-point signalized intersections, define the prototype scene of traffic flow data acquisition and transmission based on vehicle road cooperation, and introduce a neural network model and fuzzy decision technology into the design of a signal optimal control strategy. Xu *et al.* [18] study the adaptive signal timing optimization model. In view of the poor robustness of the existing traffic signal control system, an adaptive signal optimization model is established using the real-time position and speed information of vehicles. The model takes the minimum average vehicle delay as the optimization goal and the green light duration of phase as the constraint condition, uses the genetic algorithm to design the model-solving algorithm, and compares the simulation experiment to the induction control. Wang *et al.* [19] propose a multi-objective adaptive traffic signal control model based on multi-agent cooperation to optimize vehicle travel time and waiting time. Jiang *et al.* [20] propose an eco-driving system for an isolated signalized intersection under partially Connected and Automated Vehicles (CAV) environment. This system prioritizes mobility before improving fuel efficiency and optimizes the entire traffic flow by optimizing speed profiles of the connected and automated vehicles. The optimal control problem was solved using Pontryagin's Minimum Principle. Feng *et al.* [21] propose a spatio-temporal optimization traffic control model that optimizes signal lights and vehicle trajectories. Dynamic programming and nonlinear programming modeling were adopted to minimize the delay, fuel consumption, and exhaust emission when the penetration rate was 100%. Yu *et al.* [22] further propose a mixed integer linear programming model to optimize traffic signals and vehicle trajectories. In their study, the traffic flows in left turn, straight ahead, right turn and U-turn directions are considered, and the phase sequence, green light start, phase interval, cycle time, vehicle lane change behavior and vehicle arrival time are optimized together with the goal of minimizing delay. Luo *et al.* [23] study the intersection adaptive signal timing in an intelligent networked vehicle environment. First, he explores the influence of signal control variables on vehicle speed guidance, establishes an intersection traffic signal optimization model in an intelligent networked vehicle environment, and uses a dynamic programming algorithm to solve it. Xia *et al.* [24] study the coordinated control of intersection signal lights and vehicles in the intelligent network environment, considering vehicle following, traffic flow balance, intersection safety, signal phase setting and other factors, and then built a phase time traffic model for the intersection control in the mixed vehicle environment. Tang *et al.* [25] propose the bus priority control at intersections, applies a green light time loss equalization method, combines this with the data environment provided by vehicle road coordination, and aims at reducing the maximum per capita total delay at intersections. They

discuss the single point control of bus priority in a vehicle road coordination environment and the optimization of bus priority control considering intersection group filter coordination. Tao *et al.* [26], take a two one-way road intersection as an example, assuming that only a fixed proportion of vehicles can be interconnected with the intersection in real time, taking into account factors such as allowing vehicles to leave the parking line according to the fleet as much as possible and flexibly adjusting signal control, they propose a method exhausting all possible traffic sequences, and an optimization method aimed at minimizing the overall delay of intersection. Lin *et al.* [27] consider the trajectory of vehicles and intersection signal as control variables and take the minimum delay and vehicle emission as optimization objectives to build a vehicle trajectory and signal control model. Based on the above analysis, using micro traffic system simulation technology, optimization method, artificial intelligence, numerical analysis, traffic control, combining dynamic traffic organization and static traffic organization, a multi-objective optimization model of urban signalized intersection is established with the goal of maximum traffic capacity, minimum average vehicle delay and minimum vehicle density in conflict area, So as to determine the best position of parking line, the best signal period and the best signal timing index. In our study, a combination of fuzzy logic and a DEA is used to dynamically control urban traffic signals, and an optimization model of an urban traffic trunk line coordination control system is established to improve the coordination control effect.

III. DESIGN OF HIERARCHICAL FUZZY CONTROLLER OF REGIONAL INTERSECTIONS

A. Major Parameters of Fuzzy Controller

1) *Degree of Urgency of Green Light Phase*: The degree of urgency B_u of green light phase is determined by the number of vehicles B_L in line for the green light phase and the arrival rate B_{AR} of vehicles for the green light phase. B_L was calculated according to the following formula:

$$B_L = B_{L0} + C_B \quad (1)$$

where B_{L0} is the number of remaining vehicles within the detection zone after the last green light ends, and C_B is the number of vehicles arriving during the red light.

2) *Degree of Urgency in the Red Phase*: The degree of urgency of R_u of the red phase is determined by two factors: R_L -the number of queuing vehicles during the red phase and R_{AR} -the arrival rate of vehicles in the red phase. The calculation formula for R_L is as follows:

$$R_L = R_{L0} + C_R \quad (2)$$

where R_{L0} is the number of remaining vehicles within the detection zone after the last green light and C_R is the number of vehicles arriving during the red light.

3) *Degree of Urgency of Adjacent Intersection Entrance Lane Phase*: The degree of urgency N_u of the adjacent intersection entrance lane phase is determined by the number of vehicles N_L in line in that phase and the arrival rate of

TABLE I
CONTROL RULE TABLE OF GREEN LIGHT PHASE

B_u		B_{AR}				
		VS	S	M	H	VH
B_L	VS	VS	VS	S	M	H
	S	VS	S	M	M	H
	M	S	S	M	H	VH
	H	S	M	H	VH	VH
	VH	M	H	H	VH	VH

vehicles N_{AR} during the phase, among which, N_L is calculated using the following formula:

$$N_L = N_{L0} + C_N \quad (3)$$

where N_{L0} refers to the number of remaining vehicles within the detection zone after the last green light, and C_N is the number of vehicles arriving during the red light [28].

B. Module Design

1) *Detection Module for Green Light Direction in Current Intersection:* The detection module for the green light direction is used to detect the degree of urgency of vehicles in the traffic flow along the green light direction. Its input is the number of vehicles B_L in line for the current phase with a change scope of $\{0, 20\}$ and the unit of piece. The arrival rate B_{AR} of vehicles in the current phase changes within the range of $(0, 1)$. Its output is the degree of urgency B_u of vehicles for the green light direction in the current intersection with a change scope of $(0, 1)$.

a) *Fuzzification:* Fuzzify the basic domain of discourse of B_L , that is, $\{0,1,2,3,\dots,20\}$ into {very few, few, medium, many, a great many}. For convenience, it is simplified into {VS, S, M, H, VH}. The basic domain of discourse of B_{AR} , that is, $(0,1)$, is also fuzzified into {very low, low, medium, high, very high} and simplify it as {VS,S,M,H,VH}, and the basic domain of discourse of B_u , that is, $(0, 1)$ into {very light, light, medium, heavy, very heavy} and simplify as {VS, S, M, H, VH}.

b) *Selection of membership function:* The membership functions frequently used in fuzzy control include the triangle membership function, trapezoid membership function, and Gaussian membership function. The triangle membership function adopted in this study is simple, curved, with a small computing workload, saves spaces and has great sensitivity.

c) *Establishment of fuzzy control rules:* The control rules of green light phase are shown as Table I.

This fuzzy control system is based on Mamdani inference algorithm; the fuzzy statement is "IF A and B then C". For example, Control Rule No.1 in Table I can be presented as: IF B_L is VS and B_{AR} is VS then B_u is VS.

By analogy, there are 25 fuzzy control rules in total [29].

d) *Fuzzy inference relationships:* In the control rule table of the green light phase, there are 25 rules altogether, each corresponding to a fuzzy relationship. For the fuzzy statement "IF A and B then C," its relationship matrix R_i is:

$$R = (A \times B)^{T_1} \times C \quad (4)$$

TABLE II
CONTROL RULE TABLE OF RED LIGHT PHASE

R_u		R_{AR}				
		VS	S	M	H	VH
R_L	VS	VS	VS	S	M	H
	S	VS	VS	S	M	H
	M	VS	S	M	H	H
	H	S	M	M	H	VH
	VH	M	M	H	VH	VH

The corresponding fuzzy relationship for the i th control rule is:

$$R_i = (B_{Lj} \times B_{ARk})^{T_1} \times B_{ul} \quad (5)$$

where $i = 1, 2, 3, \dots, 25$ and $j, k, l = 1, 2, 3, 4, 5$; T_1 is the transfer matrix of the column vector, namely, it presents a 5×5 matrix into a 25×1 column vector; and B_{ARk} & B_{ul} are the vectors corresponding to the control rules, respectively. The total fuzzy relationships of all the 25 control rules are:

$$R = \bigcup_{i=1}^{25} R_i \quad (6)$$

2) *Detection Module for Red Light Phase in Current Intersection:* The detection module of the red-light phase is used to detect the degree of urgency of vehicles in the traffic flow for the current red light phase. Its input is R_L with a change scope of $(0, 20)$ and the unit of piece. R_{AR} changes within the scope of $(0, 1)$. Its output is the degree of urgency of vehicles in the red light phase of the current intersection with a change scope of $(0, 1)$.

a) *Fuzzification:* Fuzzify the basic domain of discourse of R_L , that is, $\{0,1,2,3,\dots,20\}$ into {very few, few, medium, many, a great many}. For convenience, it is simplified into {VS,S,M,H,VH}. Likewise, fuzzify the basic domain of discourse of R_{AR} , that is, $(0,1)$, into {very low, low, medium, high, very high } and simplify it as {VS,S,M,H,VH}, and the basic domain of discourse of R_u , that is, $(0, 1)$ into {very light, light, medium, heavy, very heavy} and simplify it as {VS,S,M,H,VH}.

b) *Selection of membership function:* The red light phase makes the same membership function selection as the green light phase, as well as the triangle membership function.

c) *Establishment of fuzzy control rules:* By summarizing the experience of experts, the control rules for the red light phase were obtained and are represented in Table II.

This fuzzy control system is based on the Mamdani inference algorithm, that is, the fuzzy statement is "IF A and B then C." For example, Control Rule No.1 in Table II can be expressed as:

IF R_L is VS and R_{AR} is VS then R_u is VS.

By analogy, there are 25 fuzzy control rules in total.

3) *Detection Module of Adjacent Intersection Entrance Lane Phase:* The detection module for the adjacent intersection entrance lane phase is used to detect the degree of urgency of traffic flow in the entrance driveway phase of the current adjacent intersections. Its input is N_L , which changes within the scope of $(0,20)$ and has a unit of piece. N_{AR} has a

TABLE III
CONTROL RULE TABLE OF ADJACENT INTERSECTION
ENTRANCE LANE PHASE

N_u		N_{AR}				
		VS	S	M	H	VH
N_L	VS	VS	VS	VS	S	M
	S	VS	VS	S	M	M
	M	VS	S	S	M	H
	H	S	S	M	H	H
	VH	M	M	H	H	VH

change scope of (0, 1). Its output is N_u with a change scope of (0, 1).

a) *Fuzzification*: Fuzzify the basic domain of discourse of N_L , that is, {0,1,2,3,...,20} into {very few, few, medium, many, a great many} simplified as {VS, S, M, H, VH}. Likewise, fuzzify the basic domain of discourse of N_{AR} , that is, (0,1), into {very low, low, medium, high, very high} and simplify it as {VS,S,M,H,VH}, and the basic domain of discourse of N_u , that is, (0, 1) into {very light, light, medium, heavy, very heavy} and simplified as {VS,S,M,H,VH}.

b) *Selection of membership function*: The adjacent intersection entrance lane phase makes the same membership function selection as the green light phase as well as the triangle membership function.

c) *Establishment of fuzzy control rules*: The control rules are obtained by summarizing the experience of experts, as shown in Table III.

This fuzzy control system is based on the Mamdani inference algorithm, that is, the fuzzy statement is "IF A and B then C." For example, Control Rule No.1 in Table III can be expressed as

IF N_L is VS and N_{AR} is VS then N_u is VS.

By analogy, there are 25 fuzzy control rules in total [30].

IV. ESTABLISHING THE TRAFFIC SIGNAL MULTI-OBJECTIVE OPTIMIZATION CONTROL MODEL

A. Average Queueing Length Model

Because the intersections are not saturated, the vehicle queueing length of the n th signal cycle can be expressed as

$$l_n = \frac{\exp\left[-\frac{4}{3}\sqrt{\lambda C q_s} \times \frac{1-x}{x}\right]}{2(1-x)} + q_n C(1-x) \quad (7)$$

where λ is the green signal ratio, q_s is the saturated traffic flow rate, x is the degree of saturation, q_n is the arrival rate of vehicles in the n th signal cycle, and C is the public signal cycle.

Assuming that the traffic flows in the up-run and down-run directions of the arterial road are q_u and q_d , respectively; thus, in a complete signal cycle, if the total up-run traffic flow along an arterial road is N , mathematically, $N = Cq_u$. Assuming that the total number of vehicle stops within a signal cycle is S , it is easy to deduce the calculation formula of stop rate h :

$$h = \frac{S}{N} \quad (8)$$

The mathematical expression of vehicle stops of up-run traffic flow in the arterial road within a certain period of time is:

$$S = q_0 + q \left[\frac{qr + q_0}{q_m - q} + r \right] \quad (9)$$

where q_m is the saturated release flow during the green light.

$$q_0 = \text{Exp} \left\{ - \left(\mu + \frac{1}{2}\mu^2 \right) \right\} \frac{1}{2} x (1-x) \quad (10)$$

$$\mu = (1-x) (q_m g)^{\frac{1}{2}} x = \frac{qT}{q_m g} \quad (11)$$

After summarizing all the above formulas, in the traffic artery, I represents the difference between the random arrival rate and average arrival rate of vehicles, while assuming that the vehicle arrival is uniform and the difference is 0, which means that $I = 0$. So

$$h = \frac{S}{N} = \frac{q \frac{qr}{q_m - q} + r}{qT} \quad (12)$$

Simplified as:

$$h = \frac{1 - g/T}{1 - q/q_m} \quad (13)$$

Considering the dual-lane green waves and summarizing the above analysis, it can be learned that the up-run stop rate h_u to travel from Intersection R_1 to Intersection R_2 is represented as:

$$h_u = \frac{1 - t_G/T}{1 - q_u/u} \quad (14)$$

Likewise, the down-run stop rate h_d from Intersection R_2 to Intersection R_1 is

$$h_d = \frac{1 - t_G/T}{q - q_d/u} \quad (15)$$

Regarding the green signal rate and the restrictions of phase difference, green signal ratio: $\lambda_{min} \leq \lambda \leq \lambda_{max}$; phase difference: $0 \leq \phi T \leq T$; cycle length: $T = \max(T_i)$ and $i = 1, 2, \dots$, T_i is the cycle of every intersection [31].

B. Calculation of Total Delay of Vehicles in Intersections

At present, the frequently used delay calculation methods include the Webster and HCM methods. The HCM formula considers the impact of the initial queue and is more suitable for the status quo of highly saturated urban roads. The specific formulae are:

$$d_i = d_1 + d_2 + d_3 \quad (16)$$

$$d_1 = \frac{0.5C(1-\lambda)^2}{1 - [\min(1, X)\lambda]} \quad (17)$$

$$d_2 = 900T \left[(X-1) + \sqrt{(X-1)^2 + \frac{8KIX}{cT}} \right] \quad (18)$$

$$d_3 = \frac{1800Q_0(1+U)T_0^2}{cT} \quad (19)$$

If $Q_0 = 0$, then $T_0 = 0$, that is $d_3 = 0$; otherwise,

$$T_0 = \min \left\{ T, \frac{Q_0}{c[1 - \min(1, X)]} \right\} \quad (20)$$

When $T_0 < T$, $U = 0$; otherwise,

$$U = 1 - \frac{cT}{Q_0[1 - \min(1, X)]} \quad (21)$$

where d_i is the average delay time per vehicle (s/veh) of the vehicle lanes divided by an entrance lane; d_1 the equilibrium delay time (s/veh); d_2 the randomly-added delay time (s/veh); d_3 the initial queue added delay time (s/veh); λ the green signal ratio; X the saturation; C the length of signal cycle (s); c the traffic capacity (veh/h); T the analytical time of duration (h); K the incremental delay correction coefficient of inductive control (for fixed-cycle signals, $K = 0.5$); I the incremental delay correction coefficient of upstream signal vehicle lane change and adjustment (here $I = 1.0$); Q_0 the number of queuing vehicles (vel) when the analytical time starts; T_0 the time with queuing vehicles (h) in the analytical time T ; and U the traffic delay feature parameter.

Therefore, the total delay of one-direction entrance lane in the intersection is

$$d_A = \frac{\sum d_i q_i}{\sum q_i} \quad (22)$$

where i represents different vehicle lanes; d_A , the total delay of one-direction entrance lanes, d_i represents the average delay per vehicle of the vehicles in the i th lanes, and q_i the vehicle arrival rate corresponding to the traffic flow of the i th lanes.

Then the total delay of intersection is:

$$D = \sum d_A q_A \quad (23)$$

where A represents different entrance lanes, D represents the total delay, and q_A represents the vehicle arrival rate corresponding to the traffic flow of entrance lane A [32].

C. Building of Traffic Signal Multi-Objective Optimal Control Model

Roads take care of time and delay the most; therefore, it has always been a research hotspot and difficult to realize low-emission and low-delay control of vehicles in traffic signal control systems. Thus, the multi-objective optimization model is built to achieve environmentally friendly traffic signal control using the model as shown below [33], [34]:

$$\min E = \sum_i \sum_k \omega_k E_{ik} \quad (24)$$

$$\min D = \sum d_A q_A \quad (25)$$

where i represents different traffic flows, k represents different pollutants ($k = 1, 2, 3$ represents VOC, CO, and NO_x , respectively) and ω_k is the weight of pollutant k .

The main idea of the utility optimization model is to first confirm all objective functions. These functions relate to all concerned problems and can be solved using methods such as the weighting method [35]:

$$\max Z = \Psi(X) \quad (26)$$

$$s.t. \Phi(X) \leq G \quad (27)$$

where Ψ is the sum function of the utility function related to the objective function.

$$\max \Psi = \sum_{i=1}^k \lambda_j \Psi_i \quad (28)$$

$$\Phi_i(x_1, x_2, \dots, x_3) \leq g_i (i = 1, 2, \dots, n) \quad (29)$$

In the formula, λ_i shall meet:

$$\sum_{k=1}^k \lambda_i = 1 \quad (30)$$

In vector form:

$$\max \Psi = \lambda^T \Psi \quad (31)$$

$$s.t. \Phi(X) \leq G \quad (32)$$

Given that delay time and emission have different units, normalization is required; thus, the following model is built:

$$PI = \alpha \times D/D_0 + \beta \times E/E_0 \quad (33)$$

where PI is the comprehensive benefit value of the function, α the weight of delayed time, β the weight of emissions, D and E the total delay time and total emissions of intersections respectively, and D_0 and E_0 the value of delay time and emission of the initial signal timing dial. For different α and β , the value of PI has different focuses. When $\alpha = 1$ and $\beta = 0$, the operation benefit of intersections depends only on the delay [36].

This objective function needs to satisfy certain constraints: the cycle length is not less than the sum of the green period and the lost time and green period not less than the effective green time, namely,

$$T_c = \sum_j (T_{g(j)} + T_{l(j)}) \leq T_{c\max} \quad (34)$$

where $T_{g(j)} \geq T_{g(j)\min}$, $20 \leq C \leq 200$, $0.3 \leq \lambda \leq 1$.

V. REALIZATION OF FASM-MDEA IN SIGNAL CONTROL, COORDINATION AND OPTIMIZATION OF URBAN INTERSECTIONS

A. Traditional Multi-Objective DEA

The main idea of the conventional multi-objective DEA includes the following five steps:

Step 1: Construct the initial population with a size of NP and calculate the fitness value of the individuals in the population. For every individual X_i in the population, carry out Steps 2-4 successively.

Step 2: According to mutation Formula (35), perform mutation on X_i .

$$V_i = X_{r1} + F \cdot (X_{r2} - X_{r3}) \quad (35)$$

where F is the size factor, the value of which changes within (0, 1). X_{r1} , X_{r2} , and X_{r3} are individuals randomly selected from the population and different from X_i .

Step 3: According to Formula (36), perform crossover on $X_i = (x_{i,1}, x_{i,2}, \dots, x_{i,n})$ and $V_i = (v_{i,1}, v_{i,2}, \dots, v_{i,n})$. Obtain the experiment vector $U_i = (u_{i,1}, u_{i,2}, \dots, u_{i,n})$. CR

is the crossover probability and values within (0,1). $rand_j \in (0, 1)$ and sn are random figure within $\{1, 2, \dots, n\}$.

$$u_{ij} = \begin{cases} v_{ij}, & \text{if } rand_j < CR \text{ or } j = sn \\ x_{ij}, & \text{otherwise} \end{cases}, j = 1, 2, \dots, n \quad (36)$$

Step 4: By comparing the domination relation between X_i and U_i , select the individuals to enter the current population. If U_i dominates X_i , replace X_i with U_i ; if X_i dominates U_i , abandon U_i directly; and if X_i and U_i do not dominate each other, add U_i into the current population.

Step 5: After all individuals in the population finish mutation, crossover, and selection, the population size grows between NP and $2NP$. At this point, a cutting operation is required, that is, after sorting the individuals in the population with the non-dominated sorting algorithm and crowding distance calculation formula, the former NP good individuals are selected for the optimization of the next generation until the termination conditions are met.

B. Fuzzy Adaptive Sorting Mutation Strategy

In mutation, FASM-MDEA adopts a sorting operation and selects the individuals with better fitness to participate in a mutation with a large probability, accelerating the convergence speed of the algorithm. However, as individuals with poor fitness are less likely to participate in the mutation, it affects the maintenance of diversity of the whole population to a certain extent. FASM-MDEA performs mutation using the fuzzy mutation Formula (37).

$$V_i = \gamma X_{best} + (1 - \gamma) * X_i + F * (X_{r1} - X_{r2}) \quad (37)$$

where X_{best} is the individual with the best fitness in the current population, and X_{r1} and X_{r2} are different and unequal to X_i . After the optimization of every generation, calculate the relative change value of the performance measurement indexes for the non-dominated solution set in the current population to the previous generation and take it as the input of the fuzzy system. Through the fuzzy system, the balance coefficient γ and size factor F of the next generation and dynamically balance the local search ability and global search capacity of the algorithm in different optimization phases in order to maintain population diversity while expediting the algorithm convergence.

Based on the sorting mutation, this study combines the feedback method of the fuzzy system and proposes a fuzzy adaptive sorting mutation strategy, shown as Formula (38):

$$V_i = \gamma X_{r1} + (1 - \gamma) * (X_{r2} + F * (X_{r3} - X_{r4})) \quad (38)$$

The selection of X_{r1} selects individuals with better fitness in the current population with a large probability. X_{r2} , X_{r3} , and X_{r4} are randomly selected individuals from the current population and are not equal to X_i ; besides, they are different from each other. The values of γ and F can be calculated by inputting into the fuzzy system the relative change value of the performance measurement indexes of the non-dominated solution set in the current population to the last generation and applied to the optimization of the next generation [37], [38].

C. Fuzzy Adaptive Sorting Mutation-Multi-Objective DEA

The fuzzy adaptive sorting mutation-multi-objective DEA (FASM-MDEA) proposed in this paper adopts a fuzzy adaptive sorting mutation strategy, uniform population initialization, and double population-based selection methods. The implementation steps are as follows.

Step 1: Input the optimization problem and relevant parameters, including the population size NP , crossover probability CR , the initial value, the maximum value F_{max} , and the minimum value F_{min} of the size factor F , the initial value, the maximum value γ_{max} , and the minimum value γ_{min} in the 1st generation of the balance coefficient γ , the number of regions L split in the uniform population initialization, and the termination conditions of the algorithm.

Step 2: Apply a uniform population initialization method, obtain the current population $Pop1$ with a size of NP and construct an empty population $Pop2$ with the same size. Calculate the fitness values of all individuals in $Pop1$.

Step 3: Starting from the $i(i = 1)$ th individual of $Pop1$, implement the following operations to all individuals X_i one by one: first, use fuzzy adaptive sorting mutation strategy and obtain the mutation vector V_i according to Formula (38); second, perform crossover on V_i and X_i as per Formula (36) and get the experiment vector U_i ; third, perform out-of-bound operation on U_i , if not exceeds the boundary value, continue; otherwise, make U_i the boundary value which is closest to it; finally, according to double population-based selection method, select U_i and X_i , and update $Pop1$ and $Pop2$.

Step 4: Complete one iteration on all individuals in the population, merge $Pop1$ and $Pop2$ into a new population with a size of $2NP$ and assign it to $Pop1$. According to the adaptive sorting mutation strategy, the relative change value of the performance measurement indexes in the non-dominated solution set in the merged population to the previous generation into the fuzzy system in order to determine the size factor F and the balance coefficient γ for the evolution of the next generation.

Step 5: Use the non-dominated sorting algorithm and crowding distance calculation formula to tailor the merged $Pop1$ and the former NP individuals as the current population $Pop1$ for the next generation evolution.

Step 6: Determine termination conditions and if they are not met, return to Step 3 and enter the next generation; otherwise, output $Pop1$ as the approximate Pareto optimal solution set to the problem and end the procedure.

VI. TRUNK TRAFFIC SIGNAL TIMING SCHEME AND SYSTEM SIMULATION ANALYSIS

The basic conditions of the selected trunk line are as follows: it is a traffic trunk line with six two-way lanes in the east, west, north, and south directions of a six intersection. The two one-way lanes are straight lanes, left-turn straight lanes, and right-turn straight lanes. The width of each lane is 3.5m. The distances between adjacent intersections were 340m, 380m, 350m, 400m, 370m and 420 m. The east-west direction is the main road direction, the north-south direction is the branch direction, and a two-phase release is adopted. The first phase is the release phase of the east-west inlet straight

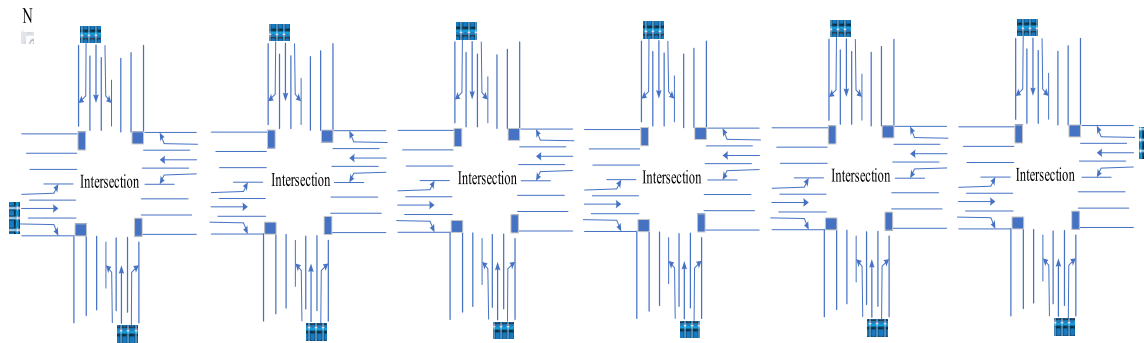


Fig. 1. Traffic arterial model of six intersections.

TABLE IV
VEHICLE CONVERSION COEFFICIENTS

Type	Car	Motorcycle	Passenger Car	Van	Big Truck	Bus	Tram
Conversion factor	1	0.5	1.2	2.0	3.0	3.0	3.5-6.0

TABLE V
DISTRIBUTION OF INTERSECTION TRAFFIC FLOW

Entrance passage	Traffic flow (pcu / h)	Flow Rate	Entrance passage	Traffic flow (pcu / h)	Flow rate
In1	1200	0.098	In8	380	0.09
In2	1050	0.245	In9	420	0.256
In3	400	0.103	In10	430	0.097
In4	360	0.093	In11	370	0.103
In5	420	0.092	In12	450	0.097
In6	410	0.091	In13	400	0.094
In7	400	0.092	In14	410	0.091

TABLE VI
TIMING SCHEME OF WEBSTER MODEL

Intersection	Signal period (s)	Green light duration (s)		Phase difference (s)
		First phase	Second phase	
S1	105	45	52	0
S2	105	43	54	23
S3	105	50	47	29
S4	105	56	41	26
S5	105	52	45	28
S6	105	54	43	27

and left-turn traffic flow, and the second phase is the release phase of the north-south inlet straight and left-turn vehicles. Fig. 1 shows the experimental trunk line model.

A. Model Solving

1) *Timing Scheme of Webster Model:* Before computing, we calibrated basic parameter information. First, all observed vehicles are converted into standard units of measurement, namely pcu, according to the vehicle conversion coefficient table in Table IV.

The saturated flow information of the road entrance is determined and the traffic conditions of urban arterial intersections

TABLE VII
TIMING SCHEME OF MAXBAND SOLUTION

Intersection		S1	S2	S3	S4	S5	S6
Signal period (s)		120	120	120	120	120	120
Green light duration (s)	First phase	67	69	61	47	59	56
	Second phase	45	43	51	65	53	56
Phase difference (s)		0	28	34	30	31	29

TABLE VIII
TIMING SCHEME OF MDEA SOLUTION

Intersection		S1	S2	S3	S4	S5	S6
Signal period (s)		130	130	130	130	130	130
Green light duration (s)	First phase	76	78	70	65	68	66
	Second phase	46	44	52	57	54	56
Phase difference (s)		0	28	34	30	31	29

TABLE IX
TIMING SCHEME OF FASM-MDEA SOLUTION

Intersection		S1	S2	S3	S4	S5	S6
Signal period (s)		130	130	130	130	130	130
Green light duration (s)	First phase	72	79	74	69	72	74
	Second phase	50	43	48	53	50	48
Phase difference (s)		0	25	32	28	30	26

are comprehensively referred to. Table V summarizes the traffic flow in the direction of each entrance lane for each intersection. The saturated flow of each through lane of the selected trunk is 1650 pcu / h, the saturated flow of each left-turn lane is 1550 pcu/h, and the saturation flow of each right-turn lane is 1450 pcu/h.

After determining the parameters on the trunk line, the next step of solving and determining the timing scheme of the traffic signal system was carried out. The common signal period and green signal ratio of the six intersections are calculated according to the Webster model method, as well the phase difference of each intersection. The timing scheme determined by the proposed FASM-MDEA is presented in Table VI.

TABLE X
COMPARISON OF EVALUATION INDICATORS OF TWO KINDS OF DEA (EAST WEST DIRECTION)

Index	From West to East			From East to West		
	MD EA	FASM-MDEA	Promotion rate	MD EA	FASM-MDEA	Promotion rate
Average delay time (s)	16.6	8.7	47.6%	19.5	8.7	55.4%
Average queue length (m)	9.5	8.7	8.4%	9.1	8.7	4.4%

TABLE XI
COMPARISON OF EVALUATION INDICATORS OF TWO KINDS OF DEA (NORTH SOUTH DIRECTION)

Index	From North to South			From South to North		
	MDE A	FASM-MDE A	Promotion rate	MDE A	FASM-MDE A	Promotion rate
Average delay time (s)	16.2	9.0	44.4%	15.9	9.3	41.5%
Average queue length (m)	10.0	9.0	10%	9.6	9.3	3.1%

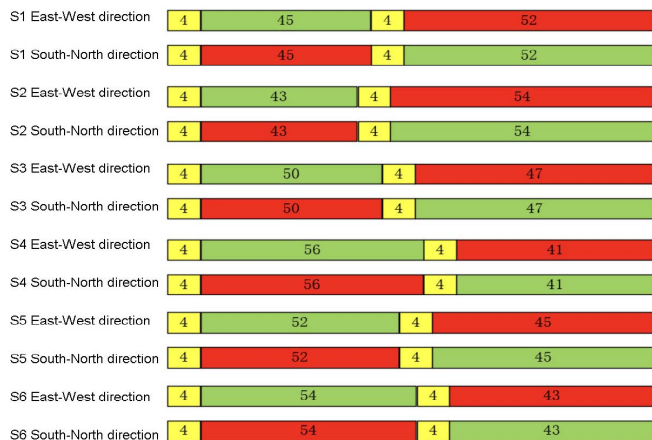


Fig. 2. Timing scheme of Webster model.

2) *MAXBAND Model Timing Scheme*: According to the MAXBAND method and the above known conditions, the traffic signal timing scheme determined by the proposed FASM-MDEA algorithm is shown in Table VII.

3) *Model Timing Scheme Based on MDEA*: The evaluation index of the traffic signal multi-objective optimization control model in this study was taken as the constituent factor of the coordinated control model of the trunk traffic system. For the new model proposed in this study, MDEA was used to solve the traffic signal timing scheme in the trunk model. The results are listed in Table VIII.

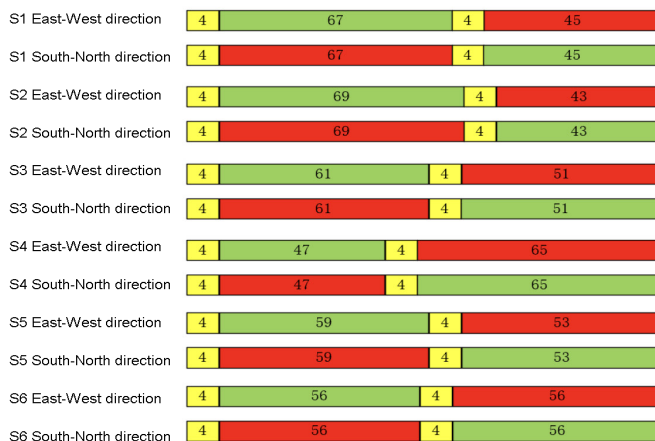


Fig. 3. MAXBAND timing scheme.

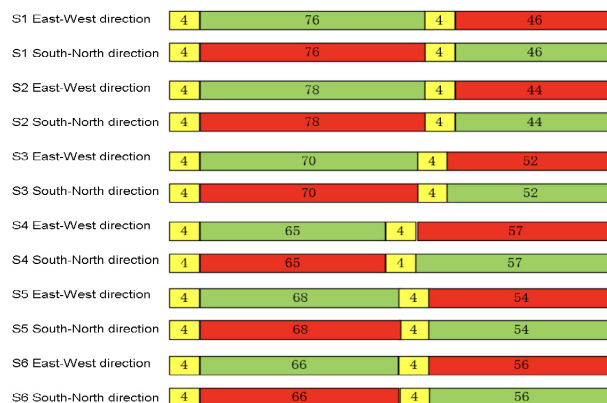


Fig. 4. Timing scheme of MDEA model.

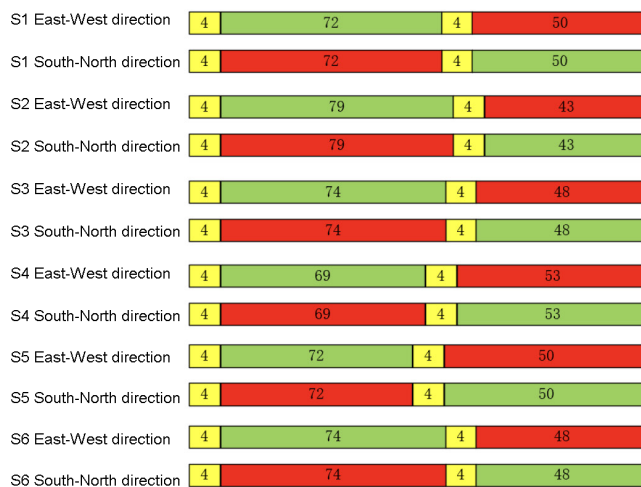


Fig. 5. Model timing scheme of FASM-MDEA algorithm.

4) *Model Timing Scheme of FASM-MDEA*: Similarly, according to the actual situation of the built traffic trunk line system, the new model is solved by FASM-MDEA with the help of the MATLAB platform, and the final signal timing scheme is determined, as shown in Table IX.

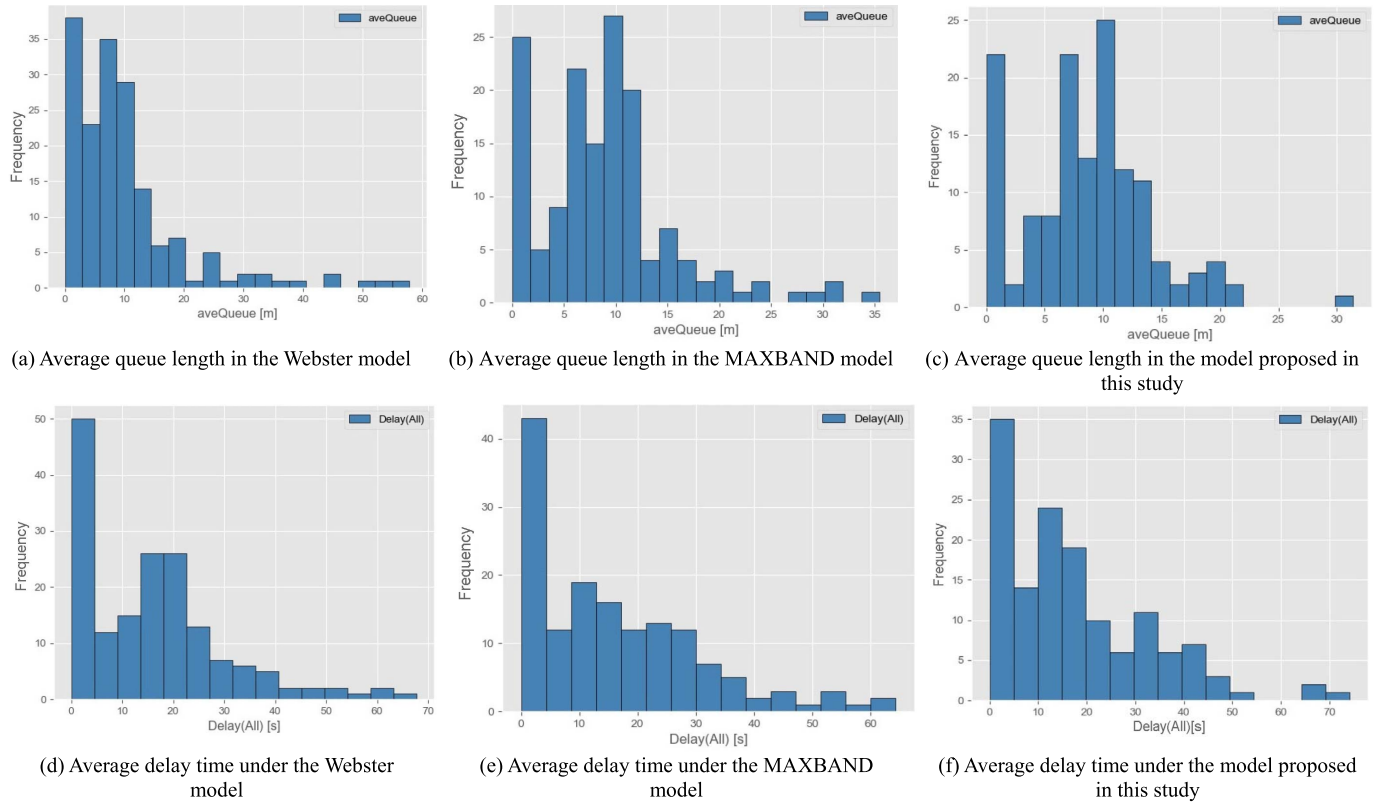


Fig. 6. Comparison of traffic evaluation indexes of three control models.

B. Analysis of Simulation Results

1) *Comparison of Three Trunk Control Models:* The micro simulation software VISSIM was used to simulate the established trunk model. In this study, the statistical data set in the time period of 3000-7200s is the collected data. The signal timing parameters obtained from the MDEA and FASM-MDEA solution models proposed in this paper are input into VISSIM, and then ten cycle times are simulated to output the statistical data of average delay time, average queue length, and vehicle exhaust emission, and the results obtained by the two model solving methods are compared and analyzed. The comparison results are presented in Tables X and XI. In the east-west direction of the experimental trunk line (trunk direction), the solution of FASM-MDEA is better than that of MDEA in terms of average delay time and average queue length, and the improvement rates from west to east are 47.6% and 8.4%, respectively; the lifting rates from east to west are 55.4% and 4.4%, respectively, from north to south are 44.4% and 10%, respectively, and from south to north are 41.5% and 3.1%, respectively, indicating that the signal timing scheme solved by the FASM-MDEA algorithm is better than that obtained by MDEA.

Finally, the Webster model, MAXBAND model, and the model proposed in this paper are set to VISSIM by using the trunk traffic signal timing parameters obtained by FASM-MDEA. Ten cycle times were simulated, and the statistical data of delay time, queue length, and vehicle exhaust emissions are output. The results obtained using several methods were compared and analyzed as shown in Fig. 6.

After ten simulation cycles, it can be seen that based on FASM-MDEA, the traffic signal timing of the trunk traffic coordination control model proposed in this paper is significantly optimized compared to the Webster model and MAXBAND model in the three performance indexes: average delay time, average queue length, and vehicle exhaust emission. After 600s-3600s simulation, the distribution histograms of the three models on the two performance indicators of the average delay time and average queue length of the traffic system are drawn. It can be seen that the distribution of the traffic timing scheme based on the FASM-MDEA model on the two indicators is small and centralized. Next, we select the data of 600s-3600s in the whole period, sum it in four directions, and calculate its average, as shown in Fig. 7.

It is clearly evident from the Fig. 7 that the proposed model has been greatly improved in terms of average queue length. In contrast, the average delay time increased negatively. Therefore, when using FASM-MDEA to solve the trunk traffic signal timing scheme, the trunk traffic system coordination control model proposed in this paper is better than other models, which is more helpful in alleviating traffic congestion and improving urban air quality.

This model effectively describes the synergistic relationship of the arrival flow rates for different inflow directions. Although the relationship between the parameters of the model is not specified in the prior distribution, the synergistic relationship of arrival flow rates between different flow directions is reflected in the posterior distribution (that is, the joint distribution of different parameters) through the effect of the likelihood function on the probability surface of the prior

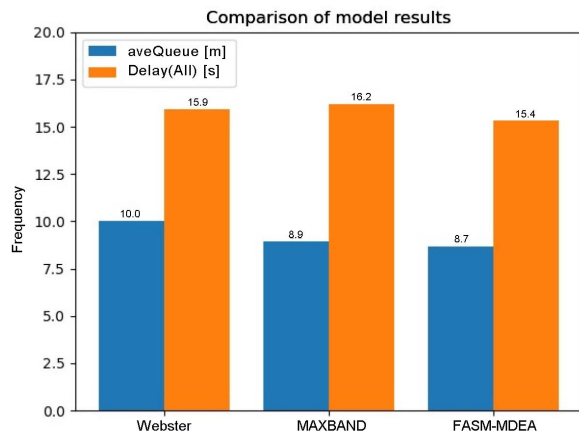


Fig. 7. Histogram of average value of traffic evaluation indexes of three control models.

distribution. In the posterior sample, it can also be found that the higher flow rate in one inflow direction corresponds to a smaller flow rate in other inflow directions. Therefore, the likelihood function or the number of arriving vehicles has an important impact on the description of the cooperative relationship.

VII. CONCLUSION AND FUTURE WORK

We took the traffic signal control of the main road of an urban intersection as the research object and reduced the average vehicle delay as the control goal, to establish common evaluation models of a traffic system, including the average delay, queue length, and vehicle exhaust emission models. By detecting the fleet length in each entrance lane, we used the fuzzy time series to predict the traffic flow in each direction of the next cycle, and we selected the appropriate timing scheme for the next cycle according to the traffic flow data to determine the optimal phase sequence arrangement. In one cycle, we used the real-time detected traffic flow as the input parameter of the adaptive fuzzy controller to obtain the green light delay of each traffic phase. Subsequently, we used the multi-objective DEA to optimize the fuzzy controller. The optimized fuzzy controller was simulated under different traffic conditions and compared to the non-optimized fuzzy controller in the same traffic environment. In addition, we studied the classical Webster model and MAXBAND model to optimize the timing of the coordinated traffic control system, proposed a new optimization method FASM-MDEA, and solved the signal timing problem of the established traffic trunk line model using the optimal timing method. The simulation results showed the intelligent control technology based on the combination of multi-objective DEA and fuzzy control effectively reduced the average delay time of passing vehicles at the intersection and adapted to the complex and changeable traffic environment.

The future work of this study is as follows:

(1) In the research scope of urban traffic control, while continuing to improve the traffic flow mathematical model and control algorithm of single intersection and urban trunk road,

we should focus on the modeling and control of urban regional traffic flow.

(2) Collaborative research between traffic control and guidance systems must be carried out to solve urban traffic problems and improve traffic efficiency.

(3) Traffic system simulation research is unrealistic to test an urban traffic signal control strategy in an actual traffic system. Therefore, the research on urban road traffic intelligent control in the virtual environment can obtain twice the result with half.

REFERENCES

- [1] K. H. N. Bui, H. Yi, H. Jung, and J. Cho, "Video-based traffic flow analysis for turning volume estimation at signalized intersections," in *Proc. Asian Conf. Intell. Inf. Database Syst.*, vol. 12034, 2020, pp. 152–162.
- [2] X. Fu, H. Gao, H. Cai, Z. Wang, and W. Chen, "How to improve urban intelligent traffic? A case study using traffic signal timing optimization model based on swarm intelligence algorithm," *Sensors*, vol. 21, no. 8, p. 2631, Apr. 2021.
- [3] H. X. Zhao, R. C. He, and N. Yin, "Modeling of vehicle CO₂ emissions and signal timing analysis at a signalized intersection considering fuel vehicles and electric vehicles," *Eur. Transp. Res. Rev.*, vol. 13, no. 1, p. 5, Jan. 2021.
- [4] J. Zhao, W. Ma, and H. Xu, "Increasing the capacity of the intersection downstream of the freeway off-ramp using presignals," *Comput.-Aided Civil Infrastruct. Eng.*, vol. 32, no. 8, pp. 674–690, Aug. 2017.
- [5] Y. Gao, Y. Liu, H. Hu, and Y. E. Ge, "Signal optimization for an isolated intersection with illegal permissive left-turning movement," *Transportmetrica B, Transp. Dyn.*, vol. 7, no. 1, pp. 928–949, Dec. 2019.
- [6] W. Anlin, D. Qiancheng, L. Guangcheng, and J. Tao, "Waiting traffic volume calculation rule of phase for self-organizing control of urban traffic signal," in *Proc. 3rd World Conf. Mech. Eng. Intell. Manuf. (WCMEIM)*, Dec. 2020, pp. 571–574.
- [7] H. Yao, X. Qu, and Y. Chen, "Research on start-up behavior and capacity at signal intersection in vehicle interconnection environment," in *Proc. Int. Conf. Transp. Develop.*, Aug. 2020, pp. 62–74.
- [8] W. Rao, J. Xia, W. Lyu, and Z. Lu, "Interval data-based k-means clustering method for traffic state identification at urban intersections," *IET Intell. Transp. Syst.*, vol. 13, no. 7, pp. 1106–1115, Jul. 2019.
- [9] L. Chai, B. Cai, W. ShangGuan, J. Wang, and H. Wang, "Connected and autonomous vehicles coordinating approach at intersection based on space-time slot," *Transportmetrica A, Transp. Sci.*, vol. 14, no. 10, pp. 929–951, Nov. 2018.
- [10] Y. Guo, C. Xiong, J. Ma, and X. Li, "Joint optimization of vehicle trajectories and intersection controllers with connected automated vehicles: Combined dynamic programming and shooting heuristic approach," *Transp. Res. C, Emerg. Technol.*, vol. 98, pp. 54–72, Jan. 2019.
- [11] S. Gong and L. Du, "Cooperative platoon control for a mixed traffic flow including human drive vehicles and connected and autonomous vehicles," *Transp. Res. B, Methodol.*, vol. 116, pp. 25–61, Oct. 2018.
- [12] D. J. Torbic, D. Cook, J. Grotheer, R. Porter, J. Gooch, and K. Kersavage, "New intersection crash prediction models for the second edition of the highway safety manual," *Transp. Res. Rec., J. Transp. Res. Board*, vol. 2676, no. 2, pp. 263–278, Sep. 2021.
- [13] B. Xu *et al.*, "Distributed conflict-free cooperation for multiple connected vehicles at unsignalized intersections," *Transp. Res. C, Emerg. Technol.*, vol. 93, pp. 322–334, Aug. 2018.
- [14] J. Huang, M.-B. Hu, R. Jiang, and M. Li, "Effect of pre-signals in a manhattan-like urban traffic network," *Phys. A, Stat. Mech. Appl.*, vol. 503, pp. 71–85, Aug. 2018.
- [15] S. Jafari, Z. Shahbazi, and Y.-C. Byun, "Improving the performance of single-intersection urban traffic networks based on a model predictive controller," *Sustainability*, vol. 13, no. 10, p. 5630, May 2021.
- [16] S. Liu, Y. Li, Y. Qiu, B. Zhang, S. Qiu, and X. Liu, "Signal timing optimization algorithm for an intersection connected with an urban expressway," *Arabian J. Sci. Eng.*, vol. 45, no. 10, pp. 8667–8684, Oct. 2020.
- [17] S. Li, T. Wang, H. Ren, X. Kong, and X. Wang, "Coordination optimization of VSL strategy on urban expressway and main road intersection signal," *IEEE Access*, vol. 8, pp. 223976–223987, 2020.
- [18] M. Xu, K. An, L. H. Vu, Z. Ye, J. Feng, and E. Chen, "Optimizing multi-agent based urban traffic signal control system," *J. Intell. Transp. Syst.*, vol. 23, no. 4, pp. 357–369, Jul. 2019.

- [19] H. Wang, P. Hu, and H. Wang, "A genetic timing scheduling model for urban traffic signal control," *Inf. Sci.*, vol. 576, pp. 475–483, Oct. 2021.
- [20] H. Jiang, J. Hu, S. An, M. Wang, and B. B. Park, "Eco approaching at an isolated signalized intersection under partially connected and automated vehicles environment," *Transp. Res. C, Emerg. Technol.*, vol. 79, pp. 290–307, Jun. 2017.
- [21] Y. Feng, C. Yu, and H. X. Liu, "Spatiotemporal intersection control in a connected and automated vehicle environment," *Transp. Res. C, Emerg. Technol.*, vol. 89, pp. 364–383, Apr. 2019.
- [22] C. Yu, Y. Feng, H. X. Liu, W. Ma, and X. Yang, "Integrated optimization of traffic signals and vehicle trajectories at isolated urban intersections," *Transp. Res. B, Methodol.*, vol. 112, pp. 89–112, Jun. 2018.
- [23] S.-D. Luo and S. Zhang, "Dynamic signal control for at-grade intersections under preliminary autonomous vehicle environment," *J. Central South Univ.*, vol. 26, no. 4, pp. 893–904, Apr. 2019.
- [24] X. H. Xia, "Adaptive traffic signal coordinated timing decision for adjacent intersections with chicken game," in *Intelligent Transport Systems—From Research and Development to the Market Uptake*, vol. 222, 2018, pp. 239–251.
- [25] T. Tang, Z. Yi, J. Zhang, and N. Zheng, "Modelling the driving behaviour at a signalised intersection with the information of remaining green time," *IET Intell. Transp. Syst.*, vol. 11, no. 9, pp. 596–603, Nov. 2017.
- [26] Z. Ge, "Reinforcement learning-based signal control strategies to improve travel efficiency at urban intersection," in *Proc. Int. Conf. Urban Eng. Manage. Sci. (ICUEMS)*, Apr. 2020, pp. 109–118.
- [27] Z. Linjie and W. Hao, "Approach to obtaining traffic volume and speed based on video-extracted trajectories," in *Proc. Int. Conf. Transp. Develop.*, Aug. 2020, pp. 140–151.
- [28] C. X. Zhu, T. Y. Wang, and J. S. Li, "Research of intersection traffic signal control and simulation based on fuzzy logic," *IOP Conf. Ser., Earth Environ. Sci.*, vol. 153, no. 3, 2018, Art. no. 032055.
- [29] R. Huang, J. M. Hu, Y. S. Huo, and X. Pei, "Cooperative multi-intersection traffic signal control based on deep reinforcement learning," in *Proc. 19th COTA Int. Conf. Transp. Prof.*, 2019, pp. 2959–2970.
- [30] S. Park, E. Han, S. Park, H. Jeong, and I. Yun, "Deep Q-network-based traffic signal control models," *PLoS ONE*, vol. 16, no. 9, Sep. 2021, Art. no. e0256405.
- [31] H. Jia, Y. Lin, Q. Luo, Y. Li, and H. Miao, "Multi-objective optimization of urban road intersection signal timing based on particle swarm optimization algorithm," *Adv. Mech. Eng.*, vol. 11, no. 4, Apr. 2019, Art. no. 168781401984249.
- [32] X. Li and J.-Q. Sun, "Signal multiobjective optimization for urban traffic network," *IEEE Trans. Intell. Transp. Syst.*, vol. 19, no. 11, pp. 3529–3537, Nov. 2018.
- [33] J. Navratil, K. Picha, S. Martinat, P. C. Nathanael, K. Tureckova, and A. Holesinska, "Resident's preferences for urban brownfield revitalization: Insights from two Czech cities," *Land Use Policy*, vol. 76, pp. 224–234, Jul. 2018, doi: [10.1016/j.landusepol.2018.05.013](https://doi.org/10.1016/j.landusepol.2018.05.013).
- [34] O. A. Arqub, M. Al-Smadi, S. Momani, and T. Hayat, "Numerical solutions of fuzzy differential equations using reproducing kernel Hilbert space method," *Soft Comput.*, vol. 20, no. 8, pp. 3283–3302, Aug. 2016.
- [35] J. Liu, Y. Jia, Y. Wang, and J. Wang, "Cumulative energy consumption analysis of signal intersections based on improved genetic algorithm," in *Proc. IEEE Int. Conf. Artif. Intell. Inf. Syst. (ICAIS)*, Mar. 2020, pp. 540–543.
- [36] Y. Qian, J. Zeng, N. Wang, J. Zhang, and B. Wang, "A traffic flow model considering influence of car-following and its echo characteristics," *Nonlinear Dyn.*, vol. 89, no. 2, pp. 1099–1109, Jul. 2017.
- [37] O. A. Arqub, "Adaptation of reproducing kernel algorithm for solving fuzzy Fredholm–Volterra integrodifferential equations," *Neural Comput. Appl.*, vol. 28, no. 7, pp. 1591–1610, Jul. 2017, doi: [10.1007/S00521-015-2110-X](https://doi.org/10.1007/S00521-015-2110-X).
- [38] D. Formanowicz, A. Sackmann, A. Kozak, J. Błażewicz, and P. Formanowicz, "Some aspects of the anemia of chronic disorders modeled and analyzed by Petri net based approach," *Bioprocess Biosyst. Eng.*, vol. 34, no. 5, pp. 581–595, Jun. 2011, doi: [10.1007/S00449-010-0507-6](https://doi.org/10.1007/S00449-010-0507-6).



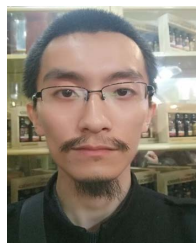
Haifeng Lin received the Ph.D. degree in forest engineering from Nanjing Forestry University, China, in 2019. He is currently an Associate Professor with the College of Information Science and Technology, Nanjing Forestry University. His current main research interests include networking, wireless communication, deep learning, pattern recognition, and the Internet of Things.



Yehong Han received the M.S. degree in management science and engineering from Shandong Normal University, Jinan, China, in 2007. She is currently an Associate Professor with the College of Information Science and Engineering, Qilu Normal University, Jinan. Her current main research interests include machine learning, pattern recognition, and the Internet of Things.



Weiwei Cai (Member, IEEE) is currently practicing at the Laboratory of Artificial Neural Networks and High-Speed Circuits, Institute of Semiconductors, Chinese Academy of Sciences, and studying at Northern Arizona University, Flagstaff, AZ, USA. Prior to that, he worked with IT industry for more than ten years in the roles of a System Architect and the Program Manager. His research interests include machine learning, deep learning, and computer vision. He is an Associate Editor of *ASP Transactions on Pattern Recognition and Intelligent Systems*. He has also served as a Guest Editor for the *Wireless Communications and Mobile Computing*, *Frontiers in Psychology*, *Computer Modeling in Engineering and Sciences*, and *Journal of Healthcare Engineering*.



Bo Jin received the B.Sc. and M.Sc. degrees from the Department of Electrical and Computer Engineering, University of Macau, China. He is currently pursuing the Ph.D. degree with the Visual Information Security Team, Institute of Systems and Robotics, Portugal. He has a wide range of research interests, especially in computers and robotics.